Intramolecular Reaction Rates of Flexible Polymers. 2. Comparison with the Renormalization Group Theory

Marta Ortiz-Repiso and Antonio Rey*

Depto. Química Física I, Facultad de Ciencias Químicas, Universidad Complutense, 28040 Madrid, Spain

Received February 19, 1998; Revised Manuscript Received August 31, 1998

ABSTRACT: The rate constants for intramolecular reactions in polymer chains, obtained through a simulation method in the previous paper, are compared with the predictions of the theory of Friedman and O'Shaughnessy, based on the renormalization group formalism. The theory describes a novel behavior of the cyclization process in certain conditions, predicting that it may be controlled by the equilibrium distribution of distances and not by the diffusion of the chain units. This prediction is confirmed by our simulation results, through the calculation of scaling laws of the rate constants with the length of the chain fragment between the reactive groups. Some quantitative theoretical predictions of the constants themselves are also checked against the simulation results. The effects of the theoretical treatment of relaxation times for internal fragments in the quantitative estimations of the rate constants is briefly discussed.

1. Introduction

In the preceding paper (hereafter referred to as paper 1), we have described the numerical calculation of intramolecular rate constants k_1 for reactive processes between functional groups attached to a single macromolecular chain. The simulation results, obtained through a Brownian dynamics algorithm,[1,2] have been compared with the quantitative predictions for these constants given by the theoretical treatment of Wilemski and Fixman,[3] using the analytical formalism of Perico and Cuniberti[4,5] and Perico and Beggiato.[6] Despite its approximations, whose effects we have tried to point out in paper 1, this theory has been widely used in the treatment of experimental data for end-to-end cyclization experiments.[7] It correctly predicts the dependence of k_1 on the capture radius of the reactive groups, the qualitative effects of excluded volume conditions over unperturbed systems, the dependence of k_1 on the chain molecular weight in θ solvents, and the qualitative effect of the chain tails on the rate constants of cyclizations involving inner units. This, together with its clear formulation, have made it almost the only theory considered in the analysis of this type of reactions.

However, other theoretical treatments have focused also on the problem of polymer cyclizations, trying to extend its scope from dilute to concentrated solutions and melts. The most complete among these theories are based upon scaling arguments and the renormalization group theory.[8,9] This approach was initiated by de Gennes, who considered two different possibilities for the way the reactive groups explore space before the reaction takes place.[10] Recently, it has been generalized by Friedman and O'Shaughnessy.[11−13] They have formulated what they call a "first principles" theory to calculate the reaction rates. Though numerical estimates for the rate constants can in principle be obtained, the main results of the theory appear in the form of general scaling laws. These relate the rate constants with the molecular weight (or chain length) of the polymer fragment comprised between the reacting groups. The scaling laws take universal simple forms in three different extreme cases.[12]

- Case I: End-to-end cyclization. The reactive units are situated at the ends of a very long chain of N units.
- Case II: End-to-interior cyclization. One of the reactive groups is at one chain end, and the other is at the chain interior. There are S units between the reactive groups. For the universal scaling laws to be valid, $S \ll N$. Thus, there is a very long tail of $(N - S)$ units without reactive groups.
- Case III: Interior-to-interior cyclization. Both reactive groups are situated in the chain interior, with two tails whose length is much longer than S. The simplest expressions appear when both tails have the same length, $\beta = (N - S)/2$, as we shall assume in this work.

For these three cases, the theory provides scaling laws for the rate constants corresponding to four types of systems: The first is *melts*, in which both excluded volume and hydrodynamic interactions (HI) are completely screened out; the system follows Rouse dynamics at short times (or free draining, Θ conditions, in the notation we have used in paper 1). Next is *Rouse plus excluded volume*, a hypothetical case without any experimental counterpart; HI are neglected (free draining conditions), but long-range intramolecular interactions which mimic excluded volume (EV) conditions are taken into account. Third is *good solvents*, where both HI and EV are considered. Finally there are Θ solvents, where HI is kept, but there are no further long-range intramolecular interactions, preserving the Gaussian statistics of the Rouse model.

As we have described in paper 1, our simulation algorithm is able to provide dynamic trajectories for long flexible chains with the different treatments of HI and solvent quality included in the four sets of conditions mentioned above. From these trajectories, the calculation of the cyclization rate constants is straighforward, independently of the position of the reactive units. Our aim in this paper is to compare the predictions of the

* To whom all correspondence should be addressed.

10.1021/ma980255l CCC: $15.00
Published on Web 10/30/1998

renormalization group theory against the numerical results of the simulation.

2. Theoretical Background

In this section we briefly summarize the main predictions of the renormalization group (RG) theory of Friedman and O'Shaughnessy. We do not try to offer a complete description of the theory, which can be found in the references from its authors.[11−13]

In contrast to the Wilemski−Fixman classical theory, where the cyclization process is mainly supposed to be controlled by the diffusion of the chain units (see the Introduction section in paper 1 and ref 5 for a further clarification on this point), the RG theory distinguishes two different regimes. One of them, termed *diffusion controlled* (DC), is equivalent to the classical assumption. The rate constant k_1 is directly related to the longest relaxation time τ_S of the fragment of S units bracketed by the reactive groups. The second regime is termed *law of mass action controlled* (LMA). Here, the rate constant is supposed to be proportional to the equilibrium contact probability, i.e., to the value of the equilibrium distribution function of the chain at short distances. In general, these two types of processes compete. The value of the rate constant could be given by something like $1/k_1 = 1/k_1^{\mathrm{LMA}} + 1/k_1^{\mathrm{DC}}$, though one of the regimes usually dominates. The crossover between them depends on factors such as the length of the chain fragment between the reactive groups, S, or the intrinsic constant for the reaction between the active groups, once they are in close proximity. This constant is supposed to be very large in the classical theory, and in our treatment of the simulation trajectories. However, for the three extreme cases of cyclization mentioned in the Introduction, the dominant regime depends only on an exponent ω, which is given by the expression

$$\omega = \frac{d+g}{z} \tag{1}$$

Here, d is the spatial dimension, which we fix at a value of 3; z is the dynamical exponent[8] which appears in the equation $\tau_S \sim r^z$, where $r = \langle r^2 \rangle^{1/2}$ is the root-mean-square distance between the reactive groups; finally, g is the so-called correlation hole exponent,[8,14] which quantifies the reduction of the probability (with respect to unperturbed conditions) that two units of the chain meet each other. (The exponent ω is named Θ in the original references.[12,13] We use the symbol ω to avoid confusion with the ideal solvent or Θ regime.)

According to the theory,[12] $\omega > 1$ corresponds to the LMA regime, while if $\omega < 1$ the DC regime predominates. Under this situation, the derivation of scaling laws for the rate constant k_1 is really simple. In the LMA regime

$$k_1 \sim \phi_{\mathrm{eq}} \sim S^{-\nu(d+g)} = S^{-\alpha} \quad \text{(LMA)} \tag{2}$$

where ν is the Flory exponent describing the dependence of the chain dimensions on the molecular weight.[8] On the other hand, in the DC regime

$$k_1 \sim 1/\tau_S \sim S^{-z\nu} \quad \text{(DC)} \tag{3}$$

From these expressions, one can get the dependence of the rate constants on S considering the values of the different exponents involved, which depend themselves on the conditions studied for every system. The relevant values are as follows.

Table 1. Scaling Laws and Behavior for k_1 Predicted by the RG Theory under the Different Conditions and for the Cyclization Cases Considered in This Work

EV	HI	LMA	DC	ω	behavior
no	no	$k_1 \sim S^{-3/2}$	$k_1 \sim S^{-2}$	3/4	DC
no	yes	$k_1 \sim S^{-3/2}$	$k_1 \sim S^{-3/2}$	1.0	−
yes	no	I: $k_1 \sim S^{-1.93}$		I: 0.885	DC
		II: $k_1 \sim S^{-2.04}$	$k_1 \sim S^{-2.18}$	II: 0.935	DC
		III: $k_1 \sim S^{-2.18}$		III: 1.003	−
yes	yes	I: $k_1 \sim S^{-1.93}$		I: 1.091	LMA
		II: $k_1 \sim S^{-2.04}$	$k_1 \sim S^{-1.76}$	II: 1.153	LMA
		III: $k_1 \sim S^{-2.18}$		III: 1.237	LMA

- The exponent ν depends on the solvent quality alone (for infinitely dilute solutions), taking the value $\nu = {}^1/_2$ under Θ conditions and $\nu = 0.588$ under excluded volume (EV) conditions.[8]
- The exponent g depends obviously on the solvent quality. In unperturbed conditions it is always $g = 0$, since we are at the reference state of its definition. On the other case, EV conditions imply a more complicated situation. The renormalization group theory used to study the distribution function in these conditions provides different values according to the position in the chain of the fragment of S units. The more accurate estimations are[15]

case I: $g = 0.27$; case II: $g = 0.46$;
case III: $g = 0.71$ (EV)

- From these values of ν and g, the exponent α in eq 2 is readily obtained. In theta conditions, it is always α=3/2. In EV conditions, its value depends once more on the cyclization case considered:

case I: $\alpha = 1.93$; case II: $\alpha = 2.04$;
case III: $\alpha = 2.18$ (EV)

- Up to now, all the exponents whose values have been presented refer to equilibrium properties, and therefore they are independent of the consideration of HI. This is not the case for the exponent z, related to a dynamic property. In free draining (FD) conditions, i.e., neglecting hydrodynamic interactions, it takes the form[16] $z = 2 + 1/\nu$, which yields the values $z = 4$ (Θ, FD) and $z = 3.70$ (EV, FD). On the other hand, when HI is taken into account, $z = d = 3$, no matter what the solvent quality is.[8,17]

The outcome of all these exponents on the scaling laws predicted by the RG theory for DC and LMA regimes is included in Table 1 (built from the information in ref 12; some exponents are very slightly different, since we are using here more accurate estimations of the exponents g and ν). In the columns labeled LMA and DC we present the laws for the two regimes. The behavior predicted by the theory, according to the value of ω, is included in the last column of the table. In two cases, the value of ω is unity (or practically equal to one). These two cases represent a crossover situation. This fact, however, does not imply any problem for the estimation of the scaling laws. It can be observed that the exponents predicted for both regimes are identical in these cases. Thus, even though a unique regime assignment is not possible, the predicted exponent is clearly determined.

When the intramolecular process is under diffusion control, the theory goes beyond the prediction of scaling

Table 2. Theoretical Predictions for the Cyclization Rate Constants in the DC Regime, According to the RG Theory, where Values of the Universal Constants Are Given in the Text

EV	HI	k_1
no	no	I: A_1/τ_S
		II: A_2/τ_S
		III: $A_4/[\tau_S \ln(\beta/S)]$[a]
yes	no	I: B_1/τ_S
		II: B_2/τ_S

[a] β is the number of units in the free tails of case III cyclizations.

laws, and it is able to provide quantitative general expressions for the rate constant k_1 as a function of the relaxation time τ_S. These expressions are collected in Table 2. The universal constants appearing in this table have the following values:[12]

$$A_1 = 16/\pi^3; \quad A_2 = 9/\pi^3; \quad A_4 = 1/\pi; \quad B_1 = 8/\pi^3; \quad B_2 = 9/(4\pi^3)$$

The logarithmic correction including the length β of the tails in case III cyclizations has not been considered in the scaling laws of Table 1.

The quantitative predictions of the RG theory deserve a couple of comments. First, the theoretical values of the rate constants do not depend on the size of the capture radius R_0 of the reactive groups. This is at odds with other theoretical and experimental results,[3,7] and with our own simulation results (see paper 1), which clearly show this dependence. Literally, the theory considers that this radius "is much smaller than other scales in the problem",[12] and thus it does not appear in universal expressions for very long chains. Since we are dealing with finite chains, we expect that the simulation results computed with our smallest value of R_0 will be in closer agreement to these quantitative predictions.

A second interesting point concerns the time τ_S appearing in all the mathematical expressions of Table 2. In the RG theory,[12] it is defined "such as to equal the longest relaxation time of the polymer, τ_N, when S is set equal to the chain length N, i.e., $\tau_S = (S/N)^{\nu z}\tau_N$ ". We think such an expression is only an approximation in dealing with the dynamic processes involving interior groups. As we have commented on in paper 1, the dynamics of a chain fragment of S units in a chain of N beads depends not only on S and N but also on the position of the fragment along the chain contour. This fact has been very recently confirmed, both theoretically and experimentally, using copolymers in which only the dynamics of certain blocks are followed.[18,19]

In the next few sections we will check the validity of the theoretical predictions, by comparing them to our Brownian dynamics simulation results.

3. Data Reduction

The model and algorithms that allow us to obtain the intramolecular rate constants have been described in paper 1 and will not be repeated here. Also, the individual values of the rate constants were presented there.

To compare the theoretical and simulation results for k_1, we need also the relaxation times τ_S, which, according to the theory, can be calculated from the longest relaxation time τ_N of the chain with N units (see above). We have obtained these times from the trajectories, computing the correlation function for the end-to-end vector. The fitting of the resulting function to a single-exponential function provides the value of τ_N. These values are collected in Table 3, together with the exponents of the scaling laws $\tau_N \sim N^{z\nu}$. These exponents result from a weighted least-squares fitting, as it will be the case for all the scaling exponents reported in this work. As we have seen in the previous section, the theoretical values of these exponents are 2.0 (FD − Θ), 1.5 (FHI − Θ), 2.18 (FD − EV) and 1.76 (FHI − EV). Thus, there is a good agreement between these predictions and our results.

In this table we have included values corresponding to fluctuating HI, a case in which, according to the RG theory, the rate constants do not depend on τ_S (see Tables 1 and 2). Therefore, we will not use these relaxation times in the comparison of simulation and theoretical results. We have done the calculations anyway to test the validity of our numerical methods in a wide variety of situations. As we can see, we are able to obtain dynamic properties from the simulations with high accuracy, and we are confident that this accuracy can be also applied to the results for the rate constants.

To get the scaling laws, the three extreme cyclization cases assumed by the theory correspond to very long chains. We think this is not a problem for end-to-end cyclizations. For the very flexible model we have used in the simulations, the larger values of N employed in this work undoubtedly reproduce the behavior of very long macromolecules. On the other hand, in paper 1 we could appreciate how the rate constants for cyclizations of cases II and III exhibit a slow decrease when N increases, keeping S constant. As a clear example of this fact, we show in Figure 1 this evolution, for case II cyclizations, and trajectories corresponding to FD − Θ conditions. (Some data computed in this particular case for $N = 225$ are included in this figure.) The data corresponding to $S = N$ (i.e., the end-to-end cyclization rate) are also included as the first point in every plot. This way, the clear decrease in cyclization rates when going from end to interior units is clearly appreciated, together with the clear trend toward a plateau exhibited when the length of the tail ($N - S$, in this figure) increases. To the best of our knowledge, there is only one very recently published work dealing with the experimental verification of this fact.[20] Though the authors measure case III cyclizations in chains with short tails (in comparison with S), the trend toward a limiting value is evident from their results. This is also in agreement with previous theoretical estimations,[6] which further estimate that the plateau is reached (again in case III) when the length of the tails is somewhere between 0.5 and 2 times the length of the fragment between the active groups, depending on the chain stiffness and on the capture strength of the two reactive groups.

The behavior shown in Figure 1 is general for all the processes involving interior groups and allows us to obtain estimates for the limiting rate constants in the extrapolation to very long tails (or, equivalently, very long N for a given S). To try to make this procedure as systematic as possible, we have checked that the numerical data can be nicely fitted to a mathematical equation of the form

Table 3. Relaxation Times τ_N^* (in Reduced Units) for the End-to-End Vector, Obtained From the Simulations, for Chains of Different Lengths N under Different Conditions: FD, Free Draining; FHI, Fluctuating Hydrodynamic Interactions; Θ, Unperturbed Conditions; EV, Excluded Volume

N	FD − Θ	FHI − Θ	FD − EV	FHI − EV
10	3.257 ± 0.002	2.773 ± 0.005	4.74 ± 0.01	3.420 ± 0.004
25	22.9 ± 0.1	10.54 ± 0.08	33.98 ± 0.07	18.73 ± 0.07
45	80.1 ± 0.1	27.79 ± 0.05	133.9 ± 0.2	51.0 ± 0.3
75	159.2 ± 0.5	61.2 ± 0.2	384.6 ± 0.6	109.9 ± 0.5
145	662 ± 2	157.0 ± 0.5	1754 ± 6	337 ± 1
scaling law	$N^{2.052 \pm 0.001}$	$N^{1.521 \pm 0.001}$	$N^{2.201 \pm 0.001}$	$N^{1.725 \pm 0.001}$

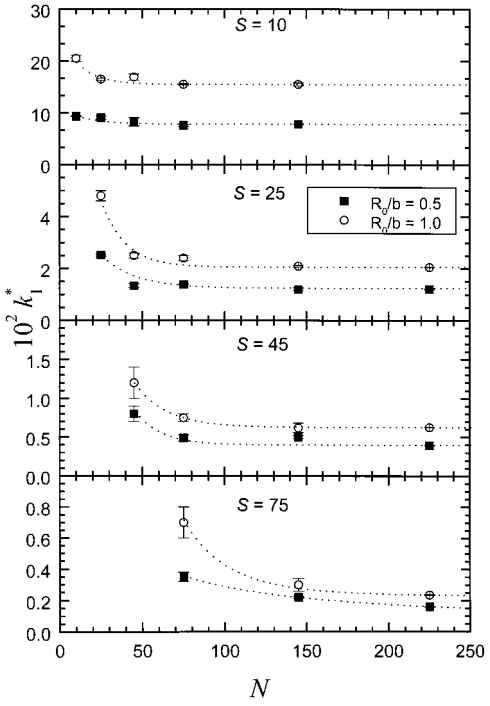

Figure 1. Variation of the rate constant k_1 (in reduced units) with N for end-to-interior intramolecular processes for various chain fragments of length S. Results from trajectories under FD − Θ conditions.

$$k_1 = A \exp(-BN) + C \qquad (4)$$

where A, B, and C are adjustable parameters. The lines plotted in Figure 1 are the results of these fittings to the cases included in the Figure. Thus, the value of C is the limiting rate constant we are looking for. When S is large, we do not have enough data to fit to the equation above. In these cases, we have taken the limit of k_1 as the value corresponding to the longest simulated chain. This may be just a crude estimation, but the trend of the curves makes us think it will not be far from the real value, probably with the exception of $S = 75$.

4. Scaling Laws

The values of the rate constants (for case I) and their limiting analogues (for cases II and III) computed from the simulations, together with the resulting scaling laws, are included in Table 4 for FD − Θ conditions. From the point of view of the RG theory, these conditions correspond to the experimental situation one encounters in the short time (tube) dynamics of melts. The RG theory predicts that these conditions are under the DC regime, with a scaling law $k_1 \sim S^{-2}$, far from the exponent $^3/_2$ corresponding to the LMA regime. Our results for the exponents clearly support this prediction, for the three cyclization classes. (We have only omitted the values of $N = 10$ in case I process from the fittings to extract the scaling laws. Its behavior clearly departs from the general linear trend in the log−log plot used to extract the scaling behavior, due to its short length.) Accordingly, the DC regime is clearly proved in these conditions.

Table 4. Limiting Values of k_1 (in Reduced Units) Obtained from Numerical Trajectories under FD − Θ Conditions

case	S	$10^2 k_1^*$ ($R_0/b = 0.5$)	$10^2 k_1^*$ ($R_0/b = 1.0$)
I	10[a]	9.37 ± 0.01	20.5 ± 0.6
end-to-end	25	2.52 ± 0.04	4.8 ± 0.2
($S = N$)	45	0.8 ± 0.1	1.2 ± 0.2
	75	0.35 ± 0.03	0.7 ± 0.1
	225	0.029 ± 0.002	0.042 ± 0.005
scaling law		$S^{-2.00 \pm 0.03}$	$S^{-2.11 \pm 0.05}$
II	10	7.6 ± 0.3	15.3 ± 0.3
end-to-interior	25	1.2 ± 0.1	2.1 ± 0.1
	45	0.45 ± 0.05	0.62 ± 0.01
	75	0.16 ± 0.01	0.24 ± 0.01
scaling law		$S^{-1.92 \pm 0.04}$	$S^{-2.11 \pm 0.02}$
III	10	5.26 ± 0.09	8.4 ± 0.3
interior-to-interior	25	0.78 ± 0.08	1.3 ± 0.2
	45	0.27 ± 0.08	0.40 ± 0.08
	75	0.07 ± 0.01	0.09 ± 0.01
scaling law		$S^{-2.11 \pm 0.06}$	$S^{-2.17 \pm 0.05}$

[a] Not included in the fit for the scaling law.

Table 5. Limiting Values of k_1 (in Reduced Units) Obtained from Numerical Trajectories under FD − EV Conditions

case	S	$10^2 k_1^*$ ($R_0/b = 0.5$)	$10^2 k_1^*$ ($R_0/b = 1.0$)
I	10	4.9 ± 0.2	12.7 ± 0.8
end-to-end	25	0.8 ± 0.1	1.7 ± 0.1
($S = N$)	45	0.15 ± 0.01	0.37 ± 0.04
	75	0.072 ± 0.002	0.155 ± 0.005
scaling law		$S^{-2.10 \pm 0.02}$	$S^{-2.19 \pm 0.03}$
II	10	2.9 ± 0.1	8.7 ± 0.1
end-to-interior	25	0.33 ± 0.02	0.81 ± 0.03
	45	0.073 ± 0.005	0.188 ± 0.002
	75	0.023 ± 0.002	0.055 ± 0.007
scaling law		$S^{-2.41 \pm 0.04}$	$S^{-2.54 \pm 0.01}$
III	10	1.57 ± 0.04	4.54 ± 0.01
interior-to-interior	25	0.182 ± 0.003	0.43 ± 0.02
	45	0.045 ± 0.001	0.108 ± 0.004
	75	0.027 ± 0.003	0.061 ± 0.005
scaling law		$S^{-2.33 \pm 0.02}$	$S^{-2.29 \pm 0.01}$

There is a slightly better agreement between the theoretical predictions and the exponents calculated with the smallest capture radius, $R_0/b = 0.5$. The difference, however, is small and is probably without physical meaning.

Table 5 shows the results for FD − EV conditions. The theory predicts now (see Table 1) a DC regime for case I and case II cyclizations and a crossover regime

Table 6. Limiting Values of k_1 (in Reduced Units) Obtained from Numerical Trajectories under FHI − Θ Conditions

case	S	$10^2 k_1^*$ ($R_0/b = 0.5$)	$10^2 k_1^*$ ($R_0/b = 1.0$)
I	10	6.9 ± 0.3	17 ± 1
end-to-end	25	1.56 ± 0.08	4.2 ± 0.2
($S = N$)	45	0.59 ± 0.05	1.22 ± 0.08
	75	0.21 ± 0.02	0.45 ± 0.03
scaling law		$S^{-1.69 \pm 0.04}$	$S^{-1.81 \pm 0.04}$
II	10	5.82 ± 0.09	15.0 ± 0.1
end-to-interior	25	1.22 ± 0.04	2.7 ± 0.2
	45	0.39 ± 0.05	0.9 ± 0.1
scaling law		$S^{-1.72 \pm 0.04}$	$S^{-1.87 \pm 0.05}$
III	10	4.25 ± 0.02	8.5 ± 0.1
interior-to-interior	25	1.17 ± 0.01	1.7 ± 0.1
	45	0.43 ± 0.04	0.84 ± 0.07
scaling law		$S^{-1.51 \pm 0.08}$	$S^{-1.57 \pm 0.03}$

Table 7. Limiting Values of k_1 (in Reduced Units) Obtained from Numerical Trajectories under FHI − EV Conditions

case	S	$10^2 k_1^*$ ($R_0/b = 0.5$)	$10^2 k_1^*$ ($R_0/b = 1.0$)
I	10	3.1 ± 0.2	11.3 ± 0.8
end-to-end	25	0.58 ± 0.08	1.8 ± 0.1
($S = N$)	45	0.17 ± 0.02	0.42 ± 0.02
	75	0.056 ± 0.001	0.11 ± 0.02
scaling law		$S^{-2.00 \pm 0.03}$	$S^{-2.23 \pm 0.04}$
II	10	2.56 ± 0.03	9.2 ± 0.1
end-to-interior	25	0.25 ± 0.02	1.0 ± 0.1
	45	0.102 ± 0.001	0.316 ± 0.001
scaling law		$S^{-2.14 \pm 0.01}$	$S^{-2.21 \pm 0.01}$
III	10	1.53 ± 0.07	4.55 ± 0.06
interior-to-interior	25	0.225 ± 0.006	0.43 ± 0.01
	45	0.060 ± 0.002	0.151 ± 0.004
scaling law		$S^{-2.16 \pm 0.04}$	$S^{-2.29 \pm 0.02}$

in case III. However, the predicted scaling law is the same in all the cases, $k_1 \sim S^{-2.18}$. The exponents would present smaller values (1.93 in case I and 2.04 in case II) if the reaction would be under LMA control. The numerical exponents obtained agree with the DC regime for end-to-end cyclizations. However, we get larger estimations (up to 10%) in the other two cases. Since these are upward differences, we think the DC regime can be still validated from these results. The observed discrepancy is probably due to the approximate character of the extrapolations which have provided the limiting values of k_1.

In Table 6 we present the results for ideal solvent solutions, i.e., FHI − Θ conditions. The RG theory provides a coincidence between DC and LMA regimes in these conditions, with a unique scaling law for any cyclization process, $k_1 \sim S^{-3/2}$. The numerical values we have obtained from the simulation are always above the theoretical estimation. The separation is the largest in end-to-interior cyclizations, and the least in the interior-to-interior case. Also, the discrepancy is slightly larger when the capture radius increases. However, we do not think a very small capture radius would give a better agreement. The Wilemski−Fixman theory considers this situation under the preaveraged HI approximation (a fact that should not affect the scaling laws), and obviously predicts the DC exponent, for different capture radii. Even more, in this case the exponent of the scaling laws relating k_1 and the relaxation times to the chain length should be the same (with opposite sign). However, we correctly get the expected exponent (see Table 3) for τ_N and a different value in the rate constants, even for end-to-end cyclizations. We do not have at the moment an explanation for this discrepancy. In our previous work with shorter chains,[21] we obtained values very similar to those obtained here for Θ solutions. There is also some experimental evidence of these exponents from studies of polystyrene capped at both chain ends with pyrene (which exhibits photochemical decay due to intramolecular excimer formation) in cyclohexane (a Θ solvent for polystyrene).[7,22] However, data of k_1 that were initially reported to give an exponent in the range 1.64−1.68 were later corrected by taking into account the experimental uncertainties (mainly the polydispersity of the sample) so that they yield an exponent of 1.43, in perfect agreement with theoretical results from Perico and Cuniberti.[4] This just shows that the exponents in the scaling laws can be very sensitive to the numerical treatment of the data, though we do not think that our values are merely a numerical artifact.

Finally, in Table 7 we collect the results equivalent to real good solvent solutions, i.e., for FHI − EV conditions. This is, probably, the most interesting case from the point of view of the comparison with the RG theory we are dealing with. There are two reasons for that. First, the RG theory predicts that any of the three extreme cyclization cases in these conditions is under the LMA regime. In addition, the difference between the exponents of LMA and DC regimes is now large enough, especially for case III cyclizations (see Table 3). This is important since, as we have just described, the estimation of the exponents is somehow blurred by small uncertainties. Thus, these systems should provide the best test to evaluate the most novel predictions of the RG theory, as recognized by its authors.[12,13] The results in Table 7 seem to support the LMA against the DC regime for these systems (the exponent predicted under DC is 1.76, for the three cyclization cases). The numerical exponents are again slightly above the theoretical estimations, but the differences are much less than in the Θ systems, especially for the smallest capture radius.

The importance of this result goes beyond the validation of the RG theory predictions. If intramolecular reactions in good solvent solutions are not diffusion controlled, the theories which consider this control as a basic assumption, as happens with the Wilemski−Fixman theory,[3] could not be safely used to compare their predictions against experimental data. Again, the available experimental data do not provide a clear answer to the problem. For end-to-end cyclizations, results for polystyrene in toluene (a good solvent) yield exponents in the range 1.76−1.92, depending on the numerical treatment used.[22] Results for polycarbonates capped with phenyl groups, in different good solvents,[23] give exponents between 1.7 and 1.9. As we have said before, data for interior-to-interior cyclizations would be much more useful, since the difference between DC and LMA regimes is probably beyond the experimental fluctuations in this case. However, the first studies of this kind have focused on the effect of different tail lengths[20] and not on the size of the chain fragment between the reactive groups.

If we admit our results as a proof of the LMA regime in FHI−EV systems, we have an additional reason to revisit our comparison of simulation and theoretical results in paper 1. We saw that, in these systems, even

the partial use of simulation results in the analytical expressions of the Wilemski−Fixman theory yields very strong differences with the numerical rate constants for $R_0/b = 0.5$, while there is a considerable agreement for $R_0/b = 1.0$. After the conclusions of the previous paragraph, we cannot rule out the possibility that this latter agreement may be just a coincidence. Other considerations of HI or EV are not affected by this fact, since the RG theory predicts for them the DC regime or identical scaling laws for DC and LMA regimes.

5. Quantitative Estimates

Finally, we have performed the theoretical quantitative estimation of the rate constants, when this situation is possible, to complete the comparison between the numerical results and the predictions of the RG theory. As we saw in the Theoretical Background section, these calculations are possible for FD − Θ and FD − EV conditions. For cyclization cases I and II, the calculation depends only on universal constants A_i and B_i, whose values were given in previous sections, following the information included in ref 12. For interior-to-interior cyclizations, the calculation is not possible in EV solvents (since it corresponds to the crossover between the LMA and DC regimes). In the FD − Θ regime the calculation is possible, but the results depend on the tail lengths β (see Table 2). The corresponding expression is only valid for $\beta > S$, a condition that holds only in a few of the systems we have simulated.

To calculate the theoretical rate constants we need the values of the times τ_S, which, according to the theory, can be computed from the longest relaxation time τ_N. For case I cyclizations, $N = S$, and we can directly use the τ_N values obtained from the trajectories and contained in Table 3. In cyclizations involving inner groups, different values can be obtained for a given S, depending on the length N of the chain used to apply the relation used by the theory, $\tau_S = (S/N)^{\nu z}\tau_N$. In principle, the differences we get must be due to the statistical fluctuations in the data for τ_N, and we use the average over the different values. We have computed the ratio between the simulation rate constants, k_1^{BD}, and the RG theoretical constants, k_1^{RG}, and present this comparison graphically.

These ratios are plotted against the chain length in Figure 2 for FD − Θ systems, for the three cyclization cases. In cases I and II, we observe a nice agreement between theory and simulation for $R_0/b = 0.5$, the smallest capture radius, agreement which is lost for $R_0/b = 1.0$. We had anticipated this situation, since the theory considers R_0 as a negligible distance in comparison with the chain size. This represents a limit which is better reached for a small capture radius. When R_0/b takes its largest value in this work, the results for case II seem to indicate that a good agreement can be reached for longer chains. The results for case I, however, do not clearly support this conclusion.

Case III cyclizations seem to show a different behavior. For short chain fragments ($S = 10$), the ratios are about the same than in the two other cases. However, for $S = 25$ and $S = 45$ this result is inverted, with a better agreement between theory and experiment for the larger capture radius. We could think about two possible reasons to explain this fact. First, the presence of two tails in the chain makes it true that, for a given N and S, the limit of very long chains is first reached in case II than in case III cyclizations. Thus, we could

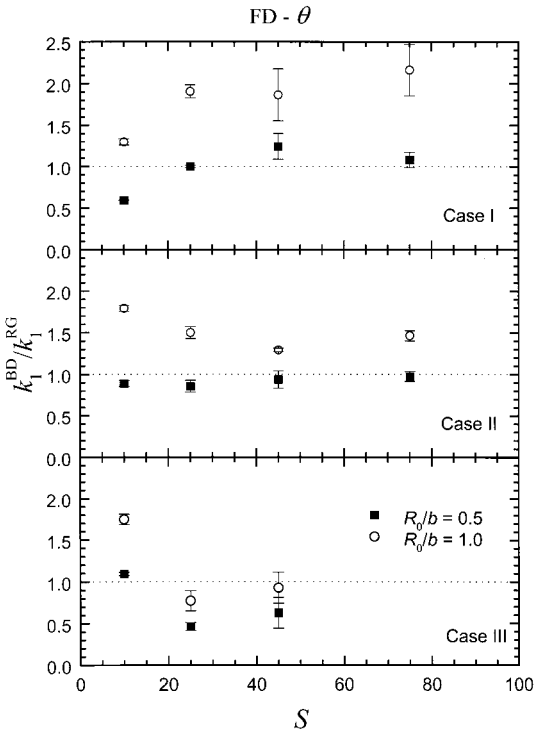

Figure 2. Ratio of simulation to RG theoretical rate constants for systems in free draining, unperturbed conditions.

be in a situation in which the simulation results obtained for finite chains are still far from the limit in which the theory can be applied. However, the fact that the scaling laws discussed in the previous section reasonably agree with the theoretical expectations, sometimes even better in case III processes than in the other two cases, could rule out this possibility. The second fact to be considered is the relation between τ_S and τ_N included in the theory. As we have already described, we believe the form used is only strictly valid for end-to-end cyclizations, but is merely an approximation for end-to-interior processes, and this approximation becomes even rougher for interior-to-interior ones. From this point of view, we cannot forget about the possibility that the weird behavior of case III results shown in Figure 2 could be partially due to this fact. Only the simulation of still much longer chains can probably solve this question. Unfortunately, these simulations are at the moment beyond our computational capabilities.

In Figure 3 we show the same ratios of rate constants for FD − EV systems, in end-to-end and end-to-interior cyclizations. Note the change of scale in the ordinate axes with respect to Figure 2. For end-to-end cyclizations, the results are the same as in Θ conditions, namely a good agreement for the small capture radius, and a deviation of around 100% for the large one. In case II, the situation is also similar, but now it is not clear whether the ratio tends toward a perfect agreement between theory and simulation or a different situation would be reached. Again, simulations of very long chains should be computed in order to clearly determine the effect of the theoretical approximation of τ_S on the quantitative estimations of the cyclization rate constants.

A different possibility we have checked in this work is to try to directly compute τ_S for chain fragments. We could use the correlation functions $\rho(\tau)$ for the vector

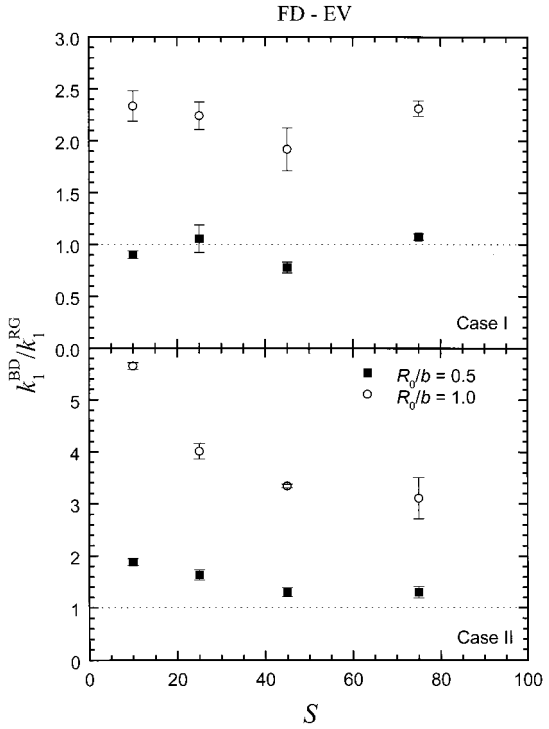

Figure 3. Ratio of simulation to RG theoretical rate constants for systems in free draining, excluded volume conditions.

joining the reactive fragments. These functions are easily obtained from the simulation, and we have used them in paper 1 in the calculation of the Wilemski–Fixman theoretical estimates of k_1. However, we discussed in paper 1 that in end-to-interior and interior-to-interior processes there is not a single dominant exponential term in these correlation functions. Of course, $\rho(\tau)$ can be still fitted to a sum of exponential terms (three, in our case), but at least two of them have equivalent amplitude factors but very different exponents. Recent experimental and theoretical work[18,19] have shown that the dynamics of arbitrary internal fragments of a polymer chain cannot be represented by a single relaxation time but are represented through a combination of several characteristic times. Given this scenario, there is not a clear definition of the time τ_S used by the RG theory in diffusion controlled intramolecular processes involving internal groups.

6. Summary and Conclusions

In this work we have used the intramolecular cyclization rate constants k_1 obtained in paper 1 to check the predictions of the renormalization group theory of Friedman and O'Shaughnessy. These predictions comprise two different levels: Scaling laws of the rate constants against the chain length and quantitative estimations of k_1.

To get the rate constants we have extracted limiting values from our simulation constants in processes involving interior groups and chain fragments of length $N \gg S$. The comparison of numerical and theoretical scaling laws validates the predictions of the RG theory, especially those concerning the conditions in which the reaction is not controlled by the diffusion of the chain units but by their equilibrium encounter probability (law of mass action control). This regime is clearly observed under good solvent conditions, when hydrodynamic interactions are included in the analysis. This confirmed novel prediction poses some doubts on the possibility that theories assuming diffusion control can be used to predict intramolecular cyclization rate constants to be compared with experimental data measured in good solvent solutions. This also includes the comparison we have carried out in paper 1 between the Wilemski–Fixman theory and our simulation results.

The RG theory quantitative estimations of k_S necessitate the values of the times τ_S, which according to the theory can be directly related to the longest relaxation time of the chain, τ_N, independently on the position of the chain fragment considered. We have checked that the theory correctly predicts the values of k_1 for end-to-end cyclizations of long finite chains, when the reactive radius of the active groups is small. In case II and, mainly, case III cyclizations, the validity of the theoretical estimations is dubious, since no unique relaxation time for the fragment considered can be defined, and therefore its relation to τ_N can be only considered as an approximation which affects the results for k_1.

Acknowledgment. This work has been partially supported by Grant PB95-0384 of the DGICYT (Ministerio de Educación y Ciencia, Spain). M.O.-R. also acknowledges a Pregraduate Fellowship (Beca Colaboración) during the Academic Year 1996/1997.

References and Notes

(1) Ermak, D. L.; McCammon, J. A. *J. Chem. Phys.* **1978**, *69*, 1352.
(2) Iniesta, A.; García de la Torre, J. *J. Chem. Phys.* **1990**, *92*, 2015.
(3) Wilemski, G.; Fixman, M. *J. Chem. Phys.* **1974**, *60*, 866; *Ibid* 878.
(4) Perico, A.; Cuniberti, C. *J. Polym. Sci., Polym. Phys. Ed.* **1977**, *15*, 1435.
(5) Cuniberti, C.; Perico, A. *Prog. Polym. Sci.* **1984**, *10*, 271.
(6) Perico, A.; Beggiato, M. *Macromolecules* **1990**, *23*, 797.
(7) Winnik, M. A. In *Photohysical and Photochemical Tools in Polymer Science*; Winnik, M. A., Ed.; NATO ASI Series: D. Reidel: Dordrecht, The Netherlands, 1986.
(8) de Gennes, P.-G. *Scaling Concepts in Polymer Physics*; Cornell University Press: Ithaca, NY, 1979.
(9) Freed, K. F. *Renormalization Group Theory of Macromolecules*; Wiley: New York, 1987.
(10) de Gennes, P.-G. *J. Chem. Phys.* **1982**, *76*, 3316.
(11) Friedman, B.; O'Shaughnessy, B. *J. Phys. II (Fr.)* **1991**, *1*, 471.
(12) Friedman, B.; O'Shaughnessy, B. *Macromolecules* **1993**, *26*, 4888.
(13) Friedman, B.; O'Shaughnessy, B. *J. Phys. II (Fr.)* **1993**, *3*, 1657.
(14) des Cloizeaux, J.; *Phys. Rev. A* **1974**, *10*, 1665.
(15) des Cloizeaux, J.; *J. Phys. (Fr.)* **1980**, *41*, 223.
(16) Oono, Y.; Freed, K. F. *J. Chem. Phys.* **1981**, *75*, 1009.
(17) Doi, M.; Edwards, S. F. *The Theory of Polymer Dynamics*; Clarendon Press: Oxford, England, 1986.
(18) Adachi, K.; Hirano, H.; Kotaka, T. *J. Non-Cryst. Solids* **1994**, *172*, 661.
(19) Adachi, K.; Hirano, H.; Freire, J. J.; Molina, L. A. *Macromolecules*, submitted for publication.
(20) Lee, S.; Winnik, M. A. *Macromolecules* **1997**, *30*, 2633.
(21) Rey, A.; Freire, J. J. *Macromolecules* **1991**, *24*, 4673.
(22) Winnik, M. A.; Redpath, A. E. C.; Paton, K.; Danhelka, J. *Polymer* **1984**, *25*, 91.
(23) Boileau, S.; Méchin, F.; Martinho, J. M. G.; Winnik, M. A. *Macromolecules* **1989**, *22*, 215.

MA980255L